

Optical simulation of a quantum thermal machine

M. H. M. Passos,^{1,2,*} Alan C. Santos,^{2,†} Marcelo S. Sarandy,^{2,‡} and J. A. O. Huguenin^{1,2,§}

¹*Instituto de Ciências Exatas, Universidade Federal Fluminense, Volta Redonda, Rio de Janeiro, Brazil*

²*Instituto de Física, Universidade Federal Fluminense,*

Av. Gal. Milton Tavares de Souza s/n, Gragoatá, 24210-346 Niterói, Rio de Janeiro, Brazil

We introduce both a theoretical and an experimental scheme for simulating a quantum thermal engine through an all-optical approach, with the behavior of the working substance and the thermal reservoirs implemented via internal degrees of freedom of a single-photon. By using polarization and propagation path, we encode two quantum bits and then implement the thermodynamical steps of an Otto cycle. To illustrate the feasibility of our proposal, we experimentally realize such simulation through an intense laser beam, evaluating heat and work at each individual step of the thermodynamical cycle. In addition, from the analysis of the entropy production during the entire cycle, we can study the amount of quantum friction produced in the Otto cycle as a function of the difference of temperature between hot and cold reservoirs. Our investigation constitutes, therefore, an *all-optical-based thermal machine* and opens perspectives for other optical simulations in quantum thermodynamics.

I. INTRODUCTION

The idealization of microscopic quantum systems allowing for extraction of work and heat is at the heart of quantum thermal engines (QTEs), quantum refrigerators [1–3], and quantum batteries [4, 5]. In analogy with its classical counterpart, a QTE has a quantum system as its *working substance*, which interacts with thermal reservoirs at different temperatures β_c and β_h . However, due the quantum nature of the working substance, one expect that the performance of a QTE may go beyond that of a classical engine [6, 7]. Concrete proposals of QTEs have been studied in recent years from different approaches [8–14]. Indeed, experimental verifications of the performance of a QTE have recently been achieved, e.g., nuclear spin systems manipulated through nuclear magnetic resonance (NMR) [15] and nitrogen-vacancy centers in diamond [16]. In general, a major difficulty for implementing QTEs in real physical systems is the high controllability required so that robustness against of decoherence is achieved. Therefore, there is great interest in designing QTEs from architectures that offer efficient control of reservoirs.

In order to simulate controllable reservoirs, we have to consider the effect of quantum channels acting on quantum information [17]. In this context, it is fundamental in our approach to take into account the optical implementation of relevant quantum channels, as amplitude damping, phase-damping, bit flip channels, among others performed by using single photons [18]. On the other hand, degrees of freedom of an intense laser beam have been widely used to simulate single-photon experiments and the results show that such procedure consists in a relevant test-bed for several quantum properties in a rather simple way [19]. Indeed, it can be shown that such systems provide realizations of quantum inequalities violations [20–22], quantum key distribution [23], teleporta-

tion [24] and quantum logical gates [25, 26]. As a further implementation of interest here, it is important to highlight the experimental simulation of open quantum systems to investigate environment-induced entanglement [27]. In this paper, we propose an all-optical-based scheme, which allows us to simulate the performance of a thermal machine in quantum mechanics and perform an experimental simulation by using degrees of freedom of an intense laser beam. We theoretically show how we can construct a quantum machine by using the phase damping channel as a thermal reservoir. We then simulate the Otto cycle for polarization of a single-photon via a linear optical circuit.

II. THE THERMAL MACHINE

Let us begin by the definition of heat and work in quantum mechanics. In general, heat and work are not quantum observables [28]. However, for the processes of interest here, either heat or work will be vanishing. In this situation, convenient expressions can be derived from the first law of thermodynamics. Indeed, by considering the internal energy $U(t)$ of a quantum system described by a density operator $\rho(t)$ at instant t as $U(t) = \text{Tr}\{H(t)\rho(t)\}$, with $H(t)$ denoting the Hamiltonian of the system, it is possible to define *work* $\delta W(t)$ and *heat* $\delta Q(t)$ for infinitesimal processes as

$$\delta W(t) = \text{Tr}\{\dot{H}(t)\rho(t)\} dt, \quad (1)$$

$$\delta Q(t) = \text{Tr}\{H(t)\dot{\rho}(t)\} dt. \quad (2)$$

Notice that $\delta W(t) > 0$ ($\delta W(t) < 0$) implies that work is being performed on (by) the system, so that its internal energy is increasing (decreasing). Similarly, when $\delta Q(t) > 0$ ($\delta Q(t) < 0$) we say that heat is being injected in (extracted from) the system.

The steps of our thermal machine is as follows. *Gap expansion step* – Initially a quantum bit (qubit) is prepared in a thermal state of the reference Hamiltonian $H_c(0) = \omega_{\text{ini}}\sigma_y$, at inverse temperature β_c . Thus, the system undergoes a unitary dynamics driven by the Hamiltonian $H_c(t) = \hbar[\omega_{\text{ini}}f(t) + \omega_{\text{fin}}g(t)]\sigma_y$, with functions $\{g, f\} : t \in \mathbb{R} \rightarrow$

*Electronic address: mhmpassos@id.uff.br

†Electronic address: ac_santos@id.uff.br

‡Electronic address: msarandy@id.uff.br

§Electronic address: jose.huguenin@id.uff.br

$g, f \in \mathbb{R}$ satisfying $g(0) = f(\tau) = 1$ and $g(\tau) = f(0) = 0$ and $|\omega_{\text{ini}}| < |\omega_{\text{fin}}|$. In this step, an amount of work is performed on/by system. *Thermalization with hot reservoir* – At this stage, the system is coupled to a thermal reservoir at inverse temperature β_{h} , thermalizing with it. Therefore, the final state at this step is a thermal state of the Hamiltonian $H_{\text{e}}(\tau)$ at inverse temperature β_{h} . In this step, the system exchange heat with the reservoir, but no work is performed. *Gap compression step* – Now, we switch off the interaction between the system and the reservoir. Thus, we drive the system by a time-dependent Hamiltonian $H_{\text{c}}(t) = \hbar[\omega_{\text{fin}}f(t) + \omega_{\text{ini}}g(t)]\sigma_y$. In this step, only work is performed on/by the system. *Thermalization with cold reservoir* – To end, the system is coupled to the cold reservoir, in which the final state is the thermal state of the Hamiltonian $H_{\text{c}}(\tau)$ at inverse temperature β_{c} . No work is performed, but heat is exchanged between the system and the cold reservoir.

From Eqs. (1) and (2) we can compute heat and work for each step of this Otto cycle (shown in Fig. 1) as

$$W_{\text{A} \rightarrow \text{B}} = -\hbar(\omega_{\text{fin}} - \omega_{\text{ini}}) \tanh(\hbar\omega_{\text{ini}}\beta_{\text{c}}), \quad (3)$$

$$Q_{\text{B} \rightarrow \text{C}} = \hbar\omega_{\text{fin}} [\tanh(\hbar\omega_{\text{ini}}\beta_{\text{c}}) - \tanh(\hbar\omega_{\text{fin}}\beta_{\text{h}})], \quad (4)$$

$$W_{\text{C} \rightarrow \text{D}} = \hbar(\omega_{\text{fin}} - \omega_{\text{ini}}) \tanh(\hbar\omega_{\text{fin}}\beta_{\text{h}}), \quad (5)$$

$$Q_{\text{D} \rightarrow \text{A}} = -\hbar\omega_{\text{ini}} [\tanh(\hbar\omega_{\text{ini}}\beta_{\text{c}}) - \tanh(\hbar\omega_{\text{fin}}\beta_{\text{h}})], \quad (6)$$

where we can derive the condition between β_{c} and β_{h} in order to get $Q_{\text{D} \rightarrow \text{A}} < 0$ as $\omega_{\text{ini}}\beta_{\text{c}} > \omega_{\text{fin}}\beta_{\text{h}}$. Such condition establishes the relation between the parameters of the reservoir and Hamiltonian as $T_{\text{h}}/T_{\text{c}} > \omega_{\text{fin}}/\omega_{\text{ini}}$.

A. Photon phase-damping channel as a thermal reservoir

We can simulate the required reservoirs for implementing a quantum machine by using a dephasing quantum channel for a single-photon. To see this, we first need to realize that our system is initially prepared in a thermal state of H_{ini} at inverse temperature β_{h} , which reads

$$\rho_{\text{ini}}^{\text{th}} = \frac{1}{2} [\mathbb{1} + \tanh(\hbar\omega_{\text{ini}}\beta_{\text{h}})\sigma_y]. \quad (7)$$

Thus, due to the contact of our system with a thermal reservoir at inverse temperature β_{h} , under action of the Hamiltonian H_{fin} , the state after thermalization will be

$$\rho_{\text{fin}}^{\text{th}} = \frac{1}{2} [\mathbb{1} + \tanh(\hbar\omega_{\text{fin}}\beta_{\text{h}})\sigma_y]. \quad (8)$$

Thus, the reservoir just changes the off-diagonal elements of the initial state, from $\tanh(\hbar\omega_{\text{ini}}\beta_{\text{h}})$ to $\tanh(\hbar\omega_{\text{fin}}\beta_{\text{h}})$. On the other hand, given a density matrix ρ with elements ρ_{nm} , we know that a phase-damping channel acts over the elements ρ_{01} and ρ_{10} as $\rho_{01} \rightarrow \rho_{01}e^{-\gamma\tau}$ and $\rho_{10} \rightarrow \rho_{10}e^{-\gamma\tau}$, respectively, where γ is the dephasing rate and τ is the total time interval of interaction of our system with the decohering reservoir. To conclude, by applying this map to the state $\rho_{\text{ini}}^{\text{th}}$ we have $\tanh(\hbar\omega_{\text{ini}}\beta_{\text{c}}) \rightarrow e^{-\gamma\tau} \tanh(\hbar\omega_{\text{ini}}\beta_{\text{c}})$, so that we can adjust the parameters $\gamma\tau$ to get the parameter β_{h} from

$$\hbar\omega_{\text{fin}}\beta_{\text{h}} = \text{arctanh} [e^{-\gamma\tau} \tanh(\hbar\omega_{\text{ini}}\beta_{\text{c}})]. \quad (9)$$

Thus, one can use the phase-damping channel to simulate the thermal reservoir in a heat engine, where we set the parameter $\gamma\tau$ to encode the hot reservoir temperature.

In several schemes of QTEs [8–14], both steps of compression and expansion are performed by slow (adiabatic) unitary evolution, so that an amount of work is performed on/by the system and no heat is exchanged. However, since any unitary dynamics suppresses the heat exchange (closed system), we can implement a fast evolution in this step [29]. In single-photon experiments we can simulate the dynamics of a quantum system through unitary operators, thus the expansion and compression steps are implemented by unitary $U_{\text{e}}(\tau)$ and $U_{\text{c}}(\tau)$, respectively, where τ is the total compression/expansion time interval (adopted to be the same in both steps). By writing the expansion/compression Hamiltonian as $H_{\text{c/e}}(t) = \hbar\omega_{\text{c/e}}(t)\sigma_y$, the unitary evolution operator is given $U_{\text{c/e}}(\bar{\omega}\tau) = e^{-i\bar{\omega}_{\text{c/e}}\tau\sigma_y}$, where we denote $\bar{\omega}_{\text{c/e}} = (1/\tau) \int_0^\tau \omega_{\text{c/e}}(t)dt$. During this evolution, an amount of work is calculated from (3) and (5), respectively.

III. EXPERIMENTAL IMPLEMENTATION

In this section we discuss about how we can encode the quantum thermal cycle discussed above in our particular system, where a general schematic representation is shown in Fig. 1. The working substance in our system, as well as any auxiliary system, is encoded in the degree of freedom of a laser beam. The qubit associated with the machine, in which we will extract/introduce heat and work, is the two independent photon polarization states $|V\rangle$ (vertical) and $|H\rangle$ (horizontal).

A. Phase-damping channel with linear optical circuits

The experimental implementation of the phase damping (PD) channels that simulates the thermal reservoirs has been performed by using linear optical circuits. In our experiment, instead of a single-photon source, we used an intense laser beam that can be described by a coherent state with a macroscopic photon number. This approach has been successfully explored in literature in different scenarios [23–27]. For this reason, we will present the experiment by using Dirac notation for polarization states once the discussion for single-photon states is straightforward. We encoded the qubit in the polarization degree of freedom and the environment in the propagation direction (path). For the polarization states, we have a two-level system, where we can associate the horizontal polarization as a ground state ($|H\rangle_{\text{S}} \equiv |0\rangle_{\text{S}}$) and the vertical polarization as an excited state ($|V\rangle_{\text{S}} \equiv |1\rangle_{\text{S}}$). In case of the propagation direction, we encoded the path also as a two-level system, with orthogonal directions, \vec{k}_0 and \vec{k}_1 , representing the reservoir ground ($|0\rangle_{\text{R}}$) and excited state ($|1\rangle_{\text{R}}$), respectively.

The scheme for the PD channel is shown in Fig. 1 (PD1, red square in the circuit). To describe the channel action on the polarization states, let us consider, without loss of generality, an incoming laser beam described by a right-circular polarized

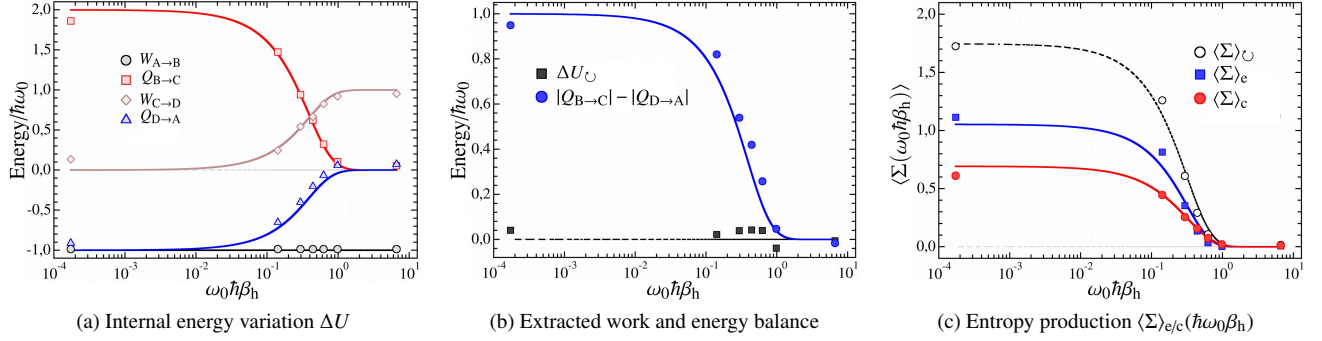


Figure 2: (2a) Heat Q and work W at each step of the Otto cycle in unities of $\hbar\omega_0$ as function of $\hbar\omega_0\beta_h$. (2b) Energy balance ΔU_{\cup} and extracted work $|Q_{B \rightarrow C}| - |Q_{D \rightarrow A}|$ for a closed cycle. (2c) Entropy production $\langle \Sigma \rangle_e$ and $\langle \Sigma \rangle_c$ associated with expansion and compression steps, respectively, as well as the entropy $\langle \Sigma \rangle_{\cup}$ yielded in a closed cycle. The working substance is initialized in the thermal state of $H_c(0)$ at temperature $k_B T_c \approx \hbar\omega/3$, where k_B is the Boltzmann constant. Continuum lines are theoretical predictions computed from Eqs. (3–6), while the points represent their respective experimental data computed from Eqs. (15) and (16). The experimental error is in the 5% range.

HWP₁₀ at 45° undoes the action of HWP₅. In the interferometer, HWP₁ at $\theta_{V2} = -\theta_V$ and HWP₂ at $\theta_{H2} = 0$ undo the action of HWP₃ at $+\theta_V$. PBS₄ regroups the arms $|0\rangle$ and $|1\rangle$, with the relative phase controlled by PZT₂ in order to obtain the initial state (circular polarization). A tomography is performed at point T_A .

IV. RESULTS AND DISCUSSION

From Eqs. (3–6) we compute heat Q and work W from the internal energy variation ΔU at each step of the Otto cycle. By using the definition of internal energy as $U = \text{Tr}\{H\rho\}$, for some reference Hamiltonian H , we evaluate U from the experimental density matrix after each thermodynamical process, which is obtained by performing quantum state tomography. Then, we have

$$W = \text{Tr}\{\rho(\tau)H(\tau) - \rho(0)H(0)\}, \quad (15)$$

$$Q = \text{Tr}\{H(\tau)[\rho(\tau_0) - \rho(\tau)]\}. \quad (16)$$

In our experimental implementation, we start from the thermal state of the Hamiltonian $H_c(0) = \hbar\omega_0\sigma_y$, with $\tanh(\hbar\omega_0\beta_c) \approx 1$ (corresponding to $\hbar\omega_0\beta_c \approx 3$). In this case, the initial state is $\rho_{\text{ini}}^{\text{th}} \approx |\psi_{\text{RL}}\rangle\langle\psi_{\text{RL}}|$. The results are presented in Fig 2. In Fig 2a, we show the internal energy variation $\Delta U/\hbar\omega_0$ as a function of $\hbar\omega_0\beta_h$ for each step of the cycle for seven different values of the inverse hot temperature β_h . In this plot, work and heat have experimentally been obtained by Eqs. (15) and (16), respectively. For a closed cycle, ΔU must be zero, which can be observed by summing up W and Q for all the curves at a fixed value of β_h . Fig. 2b shows the extracted work, quantified from difference $|Q_{B \rightarrow C}| - |Q_{D \rightarrow A}|$, due to the coupling of the system with thermal baths at different inverse temperatures β_c and β_h . As expected, the extracted work decreases as the inverse hot temperature β_h increases. In addition, note that the energy balance ΔU_{\cup} , is kept close to zero, as theoretically predicted. To study the *entropy production*, we consider the relative entropy during expansion/compression processes in a

non-equilibrium regime, which is given by [32]

$$\langle \Sigma \rangle_{e/c} = \mathcal{D}\left[U_{e/c}(\tau)\rho_{\text{th}}^{\text{cold/hot}}U_{e/c}^\dagger(\tau)\|\rho_{\text{th}}^{\text{hot/cold}}\right], \quad (17)$$

where $\mathcal{D}[A\|B] = \text{Tr}\{A \log A\} - \text{Tr}\{A \log B\}$, with $U_{e/c}(\tau)$ being the unitary evolution operator associated with the expansion/compression step and $\rho_{\text{th}}^{\text{cold/hot}}$ being the thermal state of the system associated with the cold/hot reservoir. As originally proposed, $\langle \Sigma \rangle_{e/c}$ quantifies the distance from the thermal equilibrium after an irreversible process in quantum thermodynamics. For a recent experimental implementation in NMR, see Ref. [33]. For thermodynamical cycles, the entropy production accounts for the dissipated energy during the expansion and compression steps, which may quantify *quantum friction* during the quantum evolution [34, 35]. The results are shown in Fig. 2c. Observe that the individual amounts of entropy production $\langle \Sigma \rangle_e$ and $\langle \Sigma \rangle_c$ associated with expansion and compression steps, respectively, are nonvanishing, which implies in a nonvanishing total entropy production $\langle \Sigma \rangle_{\cup}$ for thermal baths with distinct inverse temperatures β_c and β_h . Notice that, as theoretically predicted, $\langle \Sigma \rangle_{\cup}$ vanishes as β_h gets nearer β_c .

V. CONCLUSIONS

In summary, we introduced a map from a single-qubit thermal machine into a single-photon setup. The feasibility of this proposal has been experimentally tested by an all-optical experiment realized through an intense laser beam. By using the polarization degree of freedom of the laser beam, we encoded a qubit as the working substance, while the two thermal baths are simulated by an auxiliary degree of freedom, which was the propagation path in our experiment. We have then shown how different thermal baths can be implemented with optical devices, with the difference of temperatures controllable through a dimensionless parameter associated with a combination of half-wave plates. Agreement between experimental and theoretical results is remarkable, with errors within

a 5% range. It is worth emphasizing that we are proposing a simulation of thermal machine with a all-optical devices. However, our investigation opens perspectives for implementations of other protocols in quantum thermodynamics with an all-optical experimental setup, given that we can simulate two reservoirs at different temperatures with high control. In this scenario, the experimental discussion of the performance of quantum refrigerators [2, 3, 36] with optical devices and optical quantum thermometers [37, 38] are left as future research.

Acknowledgments

The Authors acknowledge financial support from the Brazilian funding agencies Conselho Nacional de Desenvolvi-

mento Científico e Tecnológico (CNPq), Fundação Carlos Chagas Filho de Amparo à Pesquisa do Estado do Rio de Janeiro (FAPERJ), Coordenação de Aperfeiçoamento de Pessoal de Nível Superior (CAPES) (Finance Code 001), and the Brazilian National Institute for Science and Technology of Quantum Information (INCT-IQ).

-
- [1] E. Geva and R. Kosloff, *J. Chem. Phys.* **96**, 3054 (1992).
 - [2] O. Abah and E. Lutz, *EPL (Europhysics Letters)* **113**, 60002 (2016).
 - [3] N. Linden, S. Popescu, and P. Skrzypczyk, *Phys. Rev. Lett.* **105**, 130401 (2010).
 - [4] R. Alicki and M. Fannes, *Phys. Rev. E* **87**, 042123 (2013).
 - [5] F. C. Binder, S. Vinjanampathy, K. Modi, and J. Goold, *New J. Phys.* **17**, 075015 (2015).
 - [6] T. D. Kieu, *Phys. Rev. Lett.* **93**, 140403 (2004).
 - [7] M. O. Scully, M. S. Zubairy, G. S. Agarwal, and H. Walther, *Science* **299**, 862 (2003).
 - [8] R. Kosloff, *The Journal of chemical physics* **80**, 1625 (1984).
 - [9] Y. Rezek and R. Kosloff, *New J. Phys.* **8**, 83 (2006).
 - [10] M. J. Henrich, F. Rempp, and G. Mahler, *Eur. Phys. J. Special Topics* **151**, 157 (2007).
 - [11] J. Geusic, E. Schulz-Du Bois, R. De Grasse, and H. Scovil, *Journal of Applied Physics* **30**, 1113 (1959).
 - [12] H. T. Quan, P. Zhang, and C. P. Sun, *Phys. Rev. E* **72**, 056110 (2005).
 - [13] J. Roßnagel *et al.*, *Science* **352**, 325 (2016).
 - [14] H. Scovil and E. Schulz-DuBois, *Phys. Rev. Lett.* **2**, 262 (1959).
 - [15] J. P. Peterson *et al.*, arXiv preprint arXiv:1803.06021 (2018).
 - [16] J. Klatzow *et al.*, arXiv preprint arXiv:1710.08716 (2017).
 - [17] M. A. Nielsen and I. L. Chuang, *Quantum Computation and Quantum Information: 10th Anniversary Edition*, 10th ed. (Cambridge University Press, New York, NY, USA, 2011).
 - [18] A. Salles *et al.*, *Phys. Rev. A* **78**, 022322 (2008).
 - [19] C. E. R. Souza, J. A. O. Huguenin, P. Milman, and A. Z. Khoury, *Phys. Rev. Lett.* **99**, 160401 (2007).
 - [20] C. V. S. Borges, M. Hor-Meyll, J. A. O. Huguenin, and A. Z. Khoury, *Phys. Rev. A* **82**, 033833 (2010).
 - [21] K. H. Kagalwala, G. Di Giuseppe, A. F. Abouraddy, and B. E. A. Saleh, *Nature Photonics* **7** (2012).
 - [22] W. F. Balthazar *et al.*, *Optics Letters* **41** (2016).
 - [23] C. E. R. Souza *et al.*, *Phys. Rev. A* **77**, 032345 (2008).
 - [24] A. Z. Khoury and P. Milman, *Phys. Rev. A* **83**, 060301 (2011).
 - [25] C. E. R. Souza and A. Z. Khoury, *Optics Express* **18** (2010).
 - [26] W. F. Balthazar and J. A. O. Huguenin, *Journal of the Optical Society of America B* **33** (2016).
 - [27] M. H. M. Passos *et al.*, *Phys. Rev. A* **97**, 022321 (2018).
 - [28] P. Talkner, E. Lutz, and P. Hänggi, *Phys. Rev. E* **75**, 050102 (2007).
 - [29] O. Abah and E. Lutz, *Phys. Rev. E* **98**, 032121 (2018).
 - [30] J. B. Altepeter, E. R. Jeffrey, and P. G. Kwiat, *Photonic State Tomography*, *Advances in Atomic, Molecular and Optical Physics* Vol. 52 (, 2005), pp. 105–159.
 - [31] R. C. Jones, *J. Opt. Soc. Am.* **31**, 488 (1941).
 - [32] S. Deffner and E. Lutz, *Phys. Rev. Lett.* **105**, 170402 (2010).
 - [33] T. B. Batalhão *et al.*, *Phys. Rev. Lett.* **115**, 190601 (2015).
 - [34] A. del Campo, J. Goold, and M. Paternostro, *Sci. Rep.* **4**, 6208 (2014).
 - [35] F. Plastina *et al.*, *Phys. Rev. Lett.* **113**, 260601 (2014).
 - [36] J. B. Brask and N. Brunner, *Phys. Rev. E* **92**, 062101 (2015).
 - [37] F. Haupt, A. Imamoglu, and M. Kroner, *Phys. Rev. Applied* **2**, 024001 (2014).
 - [38] P. P. Hofer, J. B. Brask, M. Perarnau-Llobet, and N. Brunner, *Phys. Rev. Lett.* **119**, 090603 (2017).